PB87-203105

Laboratory Analysis of Back-Corona Discharge

Southern Research Inst., Birmingham, AL

Prepared for

Environmental Protection Agency
Research Triangle Park, NC

1987

U.S. Department of Commerce
National Technical Information Service
NTIS

TECHNICAL REPORT DATA
(Please read Instructions on the reverse before completing)

1. REPORT NO. EPA/600/J-87/046	2.	3. RE PB87-203105
4. TITLE AND SUBTITLE Laboratory Analysis of Back-Corona Discharge (Journal Version)		5. REPORT DATE 1987 6. PERFORMING ORGANIZATION CODE
7. AUTHOR(S) Todd R. Snyder, P. Vann Bush, and Duane H. Pontius		8. PERFORMING ORGANIZATION REPORT NO.
9. PERFORMING ORGANIZATION NAME AND ADDRESS Southern Research Institute P. O. Box 55305 Birmingham, Alabama 35255-5305		10. PROGRAM ELEMENT NO. 11. CONTRACT/GRANT NO. CR808973
12. SPONSORING AGENCY NAME AND ADDRESS **EPA, Office of Research and Development** **Air and Energy Engineering Research Laboratory** **Research Triangle Park, NC 27711**		13. TYPE OF REPORT AND PERIOD COVERED Journal article; 8/84 - 6/86 14. SPONSORING AGENCY CODE **EPA/600/13**

15. SUPPLEMENTARY NOTES AEERL Project Officer is Leslie E. Sparks, Mail Drop 54, 919/541-2458. In: Journal of Electrostatics, Vol. 19, No. 1, pp. 101-114, 1/87.

16. ABSTRACT The paper discusses an experimental research program to characterize back-corona generation and behavior in a range of environments and geometries common to electrostatic precipitators (ESPs). A wire-parallel plate device was used to monitor the intensity and distribution of back-corona discharges. Back-corona was generated by subjecting a deposited layer of fly ash to corona current. Back-corona emissions were observed with a sensitive video camera. These observations provided new insight into the characteristics of back-corona phenomena. Conditions that were varied during the experiments included ash resistivity, corona electrode design, corona polarity, and ash-layer thickness and surface condition. The effect of pulsed energization on back-corona was also studied. Analyses of visual observations and measured distributions of corona and back-corona current allowed an assessment of the effects of back-corona emissions on ESP operating parameters.

REPRODUCED BY
U.S. DEPARTMENT OF COMMERCE
NATIONAL TECHNICAL
INFORMATION SERVICE
SPRINGFIELD, VA 22161

17. KEY WORDS AND DOCUMENT ANALYSIS

a. DESCRIPTORS	b. IDENTIFIERS/OPEN ENDED TERMS	c. COSATI Field/Group
Pollution	Pollution Control	13B
Coronas	Stationary Sources	20C
Discharge	Back-Corona Discharges	14G
Analyzing		14B
Electrostatic Precipitators		13I

18. DISTRIBUTION STATEMENT **Release to Public**	19. SECURITY CLASS *(This Report)* Unclassified	21. NO. OF PAGES 16
	20. SECURITY CLASS *(This page)* Unclassified	22. PRICE A03/F3.25

EPA Form 2220-1 (9-73)

EPA/600/J-87/046
JOURNAL ARTICLE

Journal of Electrostatics, 19 (1987) 101—114
Elsevier Science Publishers B.V., Amsterdam — Printed in The Netherlands

LABORATORY ANALYSIS OF BACK-CORONA DISCHARGE

TODD R. SNYDER, P. VANN BUSH and DUANE H. PONTIUS

Southern Research Institute, 2000 Ninth Avenue South, PO Box 55305, Birmingham, Al 35255-5305 (U.S.A.)

(Received May 17, 1985; accepted in revised form June 18, 1986)

Summary

An experimental research program was designed and performed to characterize back-corona generation and behaviour in a range of environments and geometries common to electrostatic precipitators (ESP's). A wire-parallel plate device was utilized to monitor the intensity and distribution of back-corona discharges. Back-corona was generated by subjecting a deposited layer of fly ash to corona current. Visual observations of back-corona emissions were made with a sensitive video camera. These observations provided new insight into the characteristics of back-corona phenomena. Conditions that were varied in the experiments included ash resistivity, corona electrode design, corona polarity, and ash-layer thickness and surface condition. The effect of pulsed energization on back-corona was also studied. Analyses of visual observations and measured distributions of corona- and back-corona current allowed an assessment of the effects of back-corona emissions on ESP-operating parameters.

1. Introduction

Coals which have low sulfur content have become increasingly common for use in steam generators. These coals yield fly ashes having high electrical resistivities. (For the purposes of this paper, high resistivity is defined as greater than 1×10^{11} ohm-cm.) The collection of these fly ashes with electrostatic precipitators has been the subject of numerous and widespread research and development efforts, ranging from theoretical analyses and laboratory experiments to full-scale field tests. The research has been motivated by the fact that conventional ESP's generally have significantly inferior collection efficiency for high resistivity fly ashes than for moderate-to-low resistivity fly ashes [1]. The reason for this is the degrading effects of high resistivity ash on the ESP's electrical operation.

Although fly ash layers do not strictly behave as Ohmic conductors, the relationship between allowable current density and ash resistivity is approximated by the relation:

$$j_{max} = E_b/\rho \qquad (1)$$

0304-3886/87/$03.50 © 1987 Elsevier Science Publishers B.V.

NTIS is authorized to reproduce and sell this report. Permission for further reproduction must be obtained from the copyright owner.

where E_b is the critical electric field strength for breakdown, and ρ is the resistivity of the layer. Uncertainty in the value of E_b, as well as the inaccuracy of the assumption that a fly-ash layer behaves as an Ohmic conductor, leads to uncertainty in the value of j_{max}. The inability to accurately estimate what value of current density can be attained in an ESP makes estimating the collection efficiency a matter of experience and precedent. This is a severe limitation for an industry where guarantees of collection performance are required.

The principal objectives of this research effort were to qualitatively examine the nature of back-corona discharges in a wire-plate geometry and to evaluate the onset conditions and the magnitude of back-corona emissions. The design of the experiment was intended to simulate typical ESP environments. The point-plate configuration used by several researchers [2, 3, 4] in their investigations was not selected for these measurements. The ability to characterize the current distributions in the apparatus overcame many of the possible objections to the use of wire-plate geometry. Furthermore, fly-ash layers were used in the study instead of perforated dielectrics or insulators which have been investigated by others [5]. This approach was used because recent analyses of back-corona indicated the structure of the ash layer was a determining factor in the electrical breakdown of the layer [6, 7].

2. Apparatus

A wire-plate electrode system, with wire-to-plate spacings of 12 to 15 cm, was used in a convection oven to study back-corona under various conditions. The passive collector plate was divided into 32 isolated segments, each with dimensions of 1.25 by 15 cm. Each segment was connnected to an electrometer circuit for measurement of current. Outputs from the electrometer circuits were sent to an A/D converter which rapidly and repeatedly scanned the measured currents, digitizing them for data analysis, storage, and presentation. A more detailed description of the test apparatus and sampling method has been given elsewhere [8].

Fly ash with a mass median diameter of 19.2 μm collected from a utility ESP was spread and smoothed by hand on the segmented plate to simulate the electrostatically deposited ash layer found on the plate electrode in operating precipitators. The porosity of this hand-smoothed ash layer was 60—65%. Visual observations were made with a sensitive video camera positioned to view back-corona activity on the ash layer. Parameters which were varied in the experiments included ash resistivity (induced by different operating temperatures), electrode design, polarity of corona voltage, ash-layer thickness and surface condition, and the addition of high voltage pulses to the baseline d.c. corona voltage.

3. Results

The resistivity of the fly ash used in these studies was measured using the IEEE standard method [9]. The resulting relationship between temperature and resistivity is given in Fig. 1. Measurements of the magnitude of back-corona were made by comparing the voltage–current (V–I) relationships of clean and dirty systems. One such set of V–I curves for negative polarity high voltage applied to a 0.32 cm diameter smooth electrode is shown in Fig. 2. Ash with a depth of 0.32 cm was placed on the collector electrode for these measurements. There was a large increase in current with back-corona present for all the measured voltages. It is not accurate to attribute all of the difference in current to the emissions of ions from the back-corona sites. Part of this current increase was due to the reduction in the ionic space charge resulting from emissions of corona sources of opposite polarity.

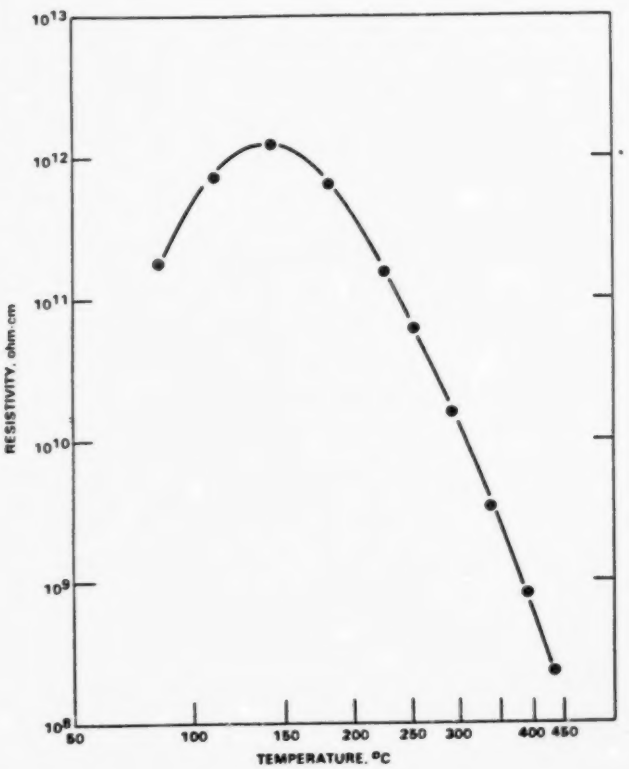

Fig. 1. Resistivity versus temperature for fly ash used in measurements and observations.

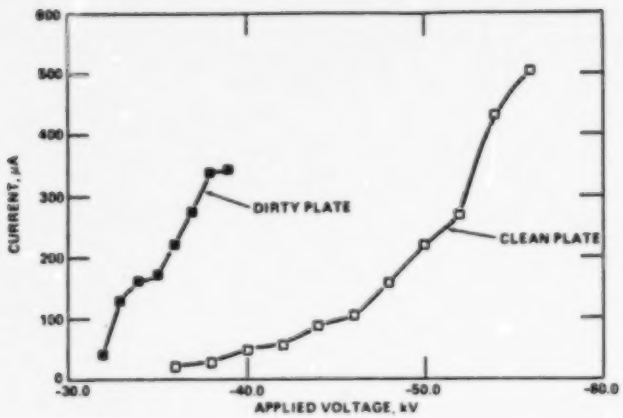

Fig. 2. Comparison of clean plate and dirty plate *V-I* curves with negative polarity and at 150°C.

The effects of the ionic space charge were demonstrated by a pair of experiments as illustrated in Fig. 3. First a pair of identical, isolated, parallel wires were energized at equal values of voltage but opposite polarity. A bipolar corona discharge, as would be present with back-corona, occurred between the two wires. In this case, the currents due to the positive and negative discharges were nearly the same. The symmetry of the apparatus resulted in almost identical distributions of positive and negative charge, so that the net space charge was essentially zero. The plane of symmetry between the two wires was an equipotential surface at ground potential. For the second experiment, a grounded metal plate was inserted in the location of that surface. The electrostatic description of the experiment was not altered thereby, but the distribution of space charge was radically changed. In the space on either side of the grounded plane, a monopolar distribution of ions was present. The results of voltage-current measurements in the two cases are shown in Fig. 4. The mixed bipolar ions permitted a much more vigorous discharge than the monopolar ion environment because of the neutralization of the ionic space charge in the bipolar experiment.

These experiments demonstrate the degree to which back-corona activity not only "feeds" on corona current, but promotes more intense primary corona emission. Visual observations of back-corona activity gave evidence of this relationship, with the intensity of the corona emissions increasing with the onset of back-corona. Other evidences of this effect were found in the measured distributions of current with and without back-corona.

A statistical quantity of particular value in interpreting current distributions was the coefficient of variation (COV) of the measured distribution. COV is the normalized standard deviation expressed as a percentage [10]:

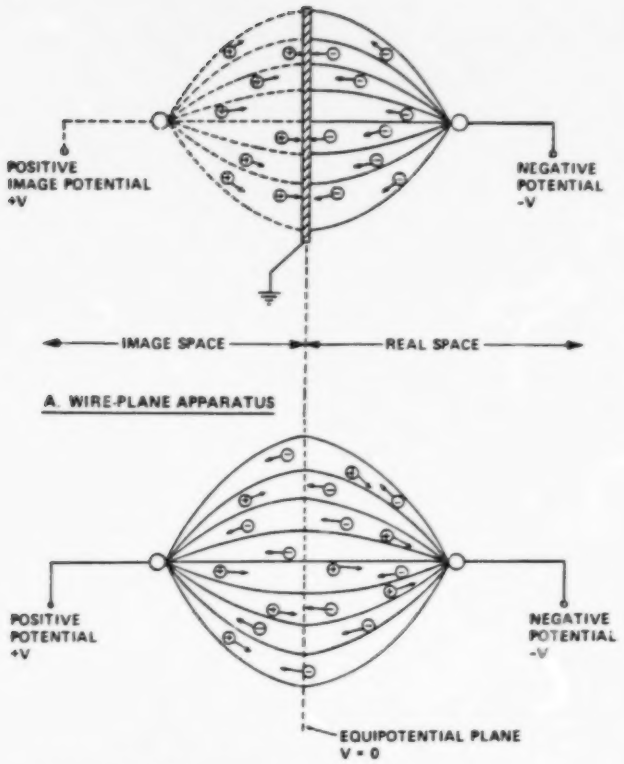

Fig. 3. Bipolar corona, space-charge neutralized (a). Twin unipolar corona (b).

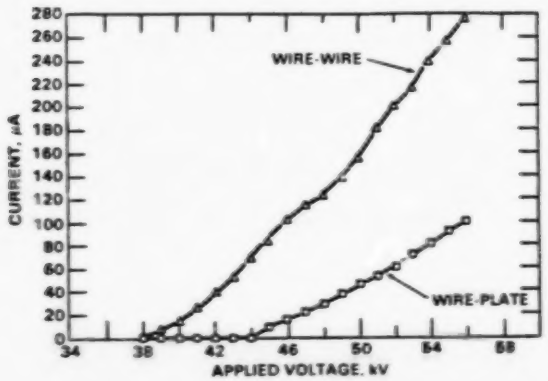

Fig. 4. Comparison of conduction characteristics of bipolar and mirror-twin unipolar corona discharges.

$$\text{COV} = (\sigma/\bar{x}) \cdot 100 \qquad (2)$$

where σ is the standard deviation of the average values of the current measured on the segments from $\bar{x}$, the mean value of current for the distribution. Current distribution measurements showed the effect of back-corona on the magnitude and uniformity of current. Output from a pair of these measurements made with a 0.32 cm ash layer is shown in Fig. 5. The behaviour of the current measured from two individual collector segments covered with a 0.32 cm ash layer is given in Fig. 6. The sudden rise in current on the collectors coincided with the onset of back-corona activity from these segments.

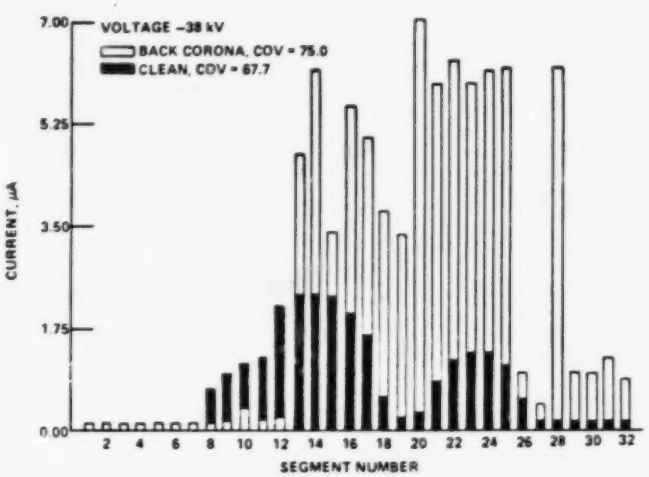

Fig. 5. Current distributions for negative corona with and without back-corona at 150°C.

Videotaped observations of the ash layer under negative ion bombardment showed the back-corona to be highly active. Rapidly shifting centers of back-corona activity were comparable in appearance to Lichtenberg figures, described by Loeb [11]. Streamers extended radially along the surface of the ash layer about two centimeters from the bright core of the discharge. Back-corona activity occurred beneath active ionization spots on the wire, indicative of a synergic relationship. Only at very high current densities did the back-corona in the layer spread to areas above which there was no observable primary corona.

Analysis of videotape still-frame progression revealed that the total elapsed time from the first appearance of a discrete center of back-corona to its extinction could be as brief as 0.06 s. The duration of an individual center of back-corona was principally dependent on the surface roughness of the ash layer. A photograph taken from the video display of back-corona

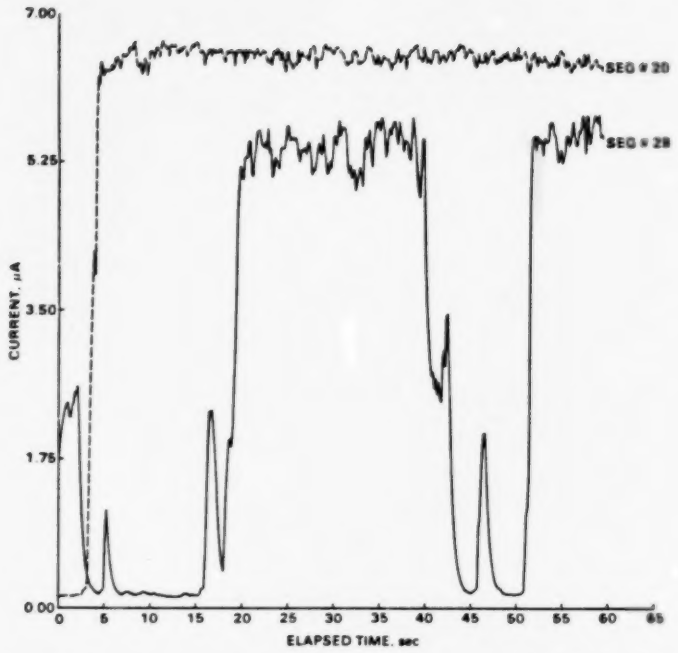

Fig. 6. Current as a function of time for two segments of an ash-covered plate at 150°C showing the onset of back-corona activity.

sites produced with a primary voltage of −40 kV in a 0.32 cm ash layer is shown in Fig. 7.

The back-corona associated with positive primary corona was different in appearance from the negative corona product, as was expected. The back-corona sites typically extended over 1/4 to 1/2 of the area and were more numerous than the back-corona sites induced by negative corona. There were no detectable streamers from each site along the ash layer, but rather a cloud of ionization appeared to penetrate within the 0.32 cm ash layer. A photograph of this type of back corona observed at a primary voltage of 46 kV is presented in Fig. 8. The effect of back-corona on the current distribution was more pronounced for the positive-polarity corona. Figure 9 is a plot of the current distribution of clean-plate and dirty-plate (0.32 cm ash layer) conditons. The current with back-corona was an order of magnitude greater than the current generated from the wire in the clean system. Plots of the COV versus voltage for measurements made with the collector electrode clean and covered with a 0.32 cm ash layer at 100 and 150°C (Fig. 10) emphasize the degree to which the back-corona degraded the current distribution on the plate. The back-corona sites caused corona

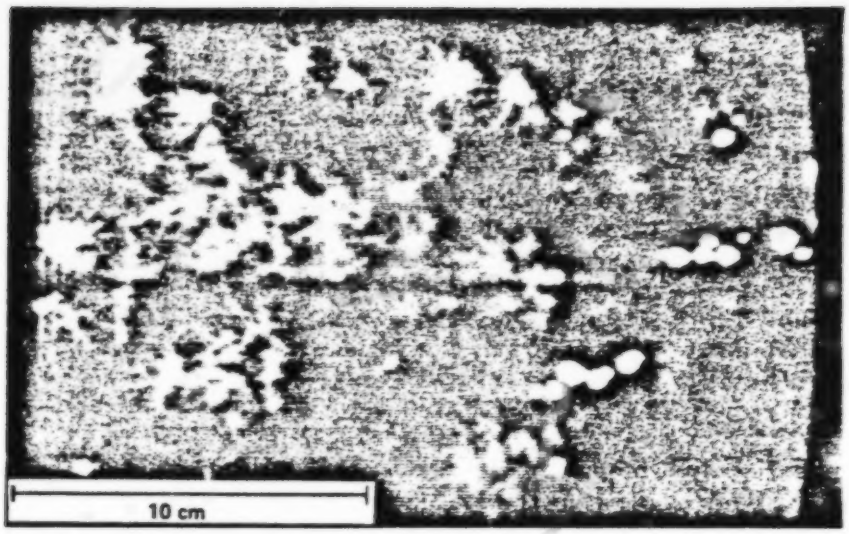

Fig. 7. Photograph of back-corona on a dust layer ($\sim 10^{12}$ Ω-cm resistivity fly ash) under negative polarity corona wire.

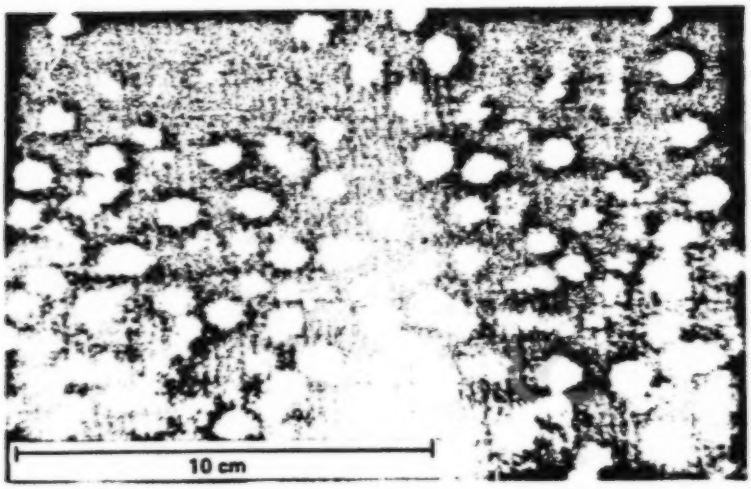

Fig. 8. Photograph of back-corona on a dust layer ($\sim 10^{12}$ Ω-cm resistivity fly ash) under positive polarity corona wire.

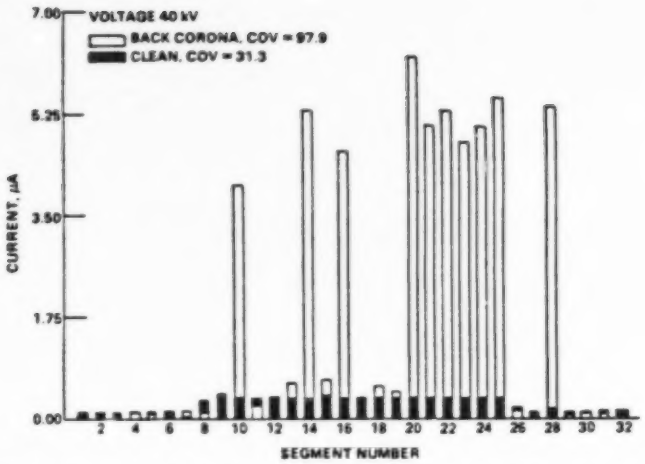

Fig. 9. Current distributions for positive corona with and without back-corona at 150°C.

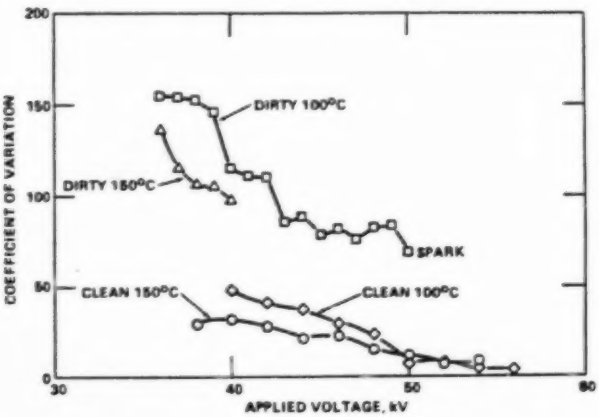

Fig. 10. Coefficient of variation versus voltage for clean and dirty plate with positive polarity corona discharges at 100 and 150°C.

streamers to develop from the discharge wire, severely limiting the operating voltage range by leading to sparking. This limitation is shown in Fig. 10 by the data measured at 100°C, where sparking occurred at 50 kV for the ash-covered plate, well below the 56 kV achievable with the collection electrode clean.

An alternate type of corona energization tested was pulsed energization, which consisted of adding a 2 μs wide pulse of -10 kV amplitude to the

negative polarity baseline voltage. Pulse frequencies from 10 to 300 Hz were tested. The smoothing effect the pulsed energization had on the primary corona distribution [12] was accompanied by a change in back-corona behaviour. For current densities comparable to those tested for simple d.c. energization, visual observations revealed that the number of active back-corona sites generated was significantly reduced for the pulsed corona. This reduction is probably attributable to the absence of stable points of corona on the wire. Comparisons of the COV measured for simple d.c. energization versus pulsed energization indicate the magnitude of the smoothing effect on the current distribution. The COV of segments 7–28

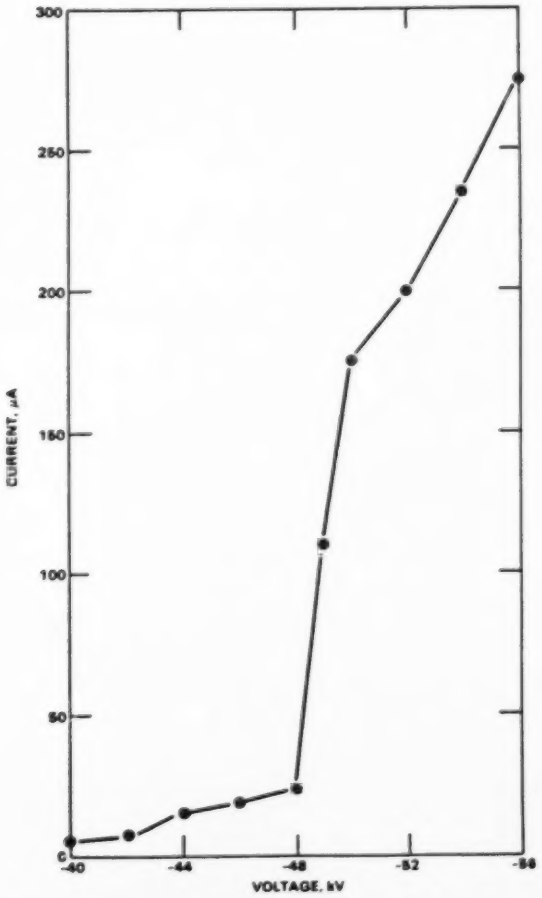

Fig. 11. Voltage-current characteristics for the ballasted electrode above the ash-covered plate at 150°C.

measured at the same total current levels decreased from 90.3 for d.c. energization to 7.3 for pulsed energization. In this same comparison, the addition of the −10 kV, 250 Hz pulse allowed the baseline d.c. voltage to reach −43.4 kV while an identical total current was generated with simple d.c. energization of −41.0 kV.

An even distribution of primary corona was seen also to affect back-corona behaviour in tests of a "ballasted" electrode [8]. The ballasting is accomplished by a porcelain enamel coating applied to the discharge electrode. The onset of corona current produced a voltage drop in this resistive layer, effectively suppressing local current until the potential reached the point at which the entire electrode length developed corona discharge. *V—I* data taken at 150°C indicated that back-corona onset occurred in a 0.32 cm ash layer between −48 kV and −49 kV as seen in Fig. 11. A chip in the porcelain ballasting layer located above segment No. 6 served as a site for intense stable corona emission. As can be seen in Fig. 12, an otherwise uniform current distribution was deformed by high current due to back-corona activity on segment No. 6. Back-corona activity in the 0.32 cm ash layer was localized to the area directly below the active ionization spot. Regions of the plate beneath evenly distributed primary corona did not exhibit back-corona. Stable ionization points generated the high local current densities thought to be the critical factor in back-corona onset.

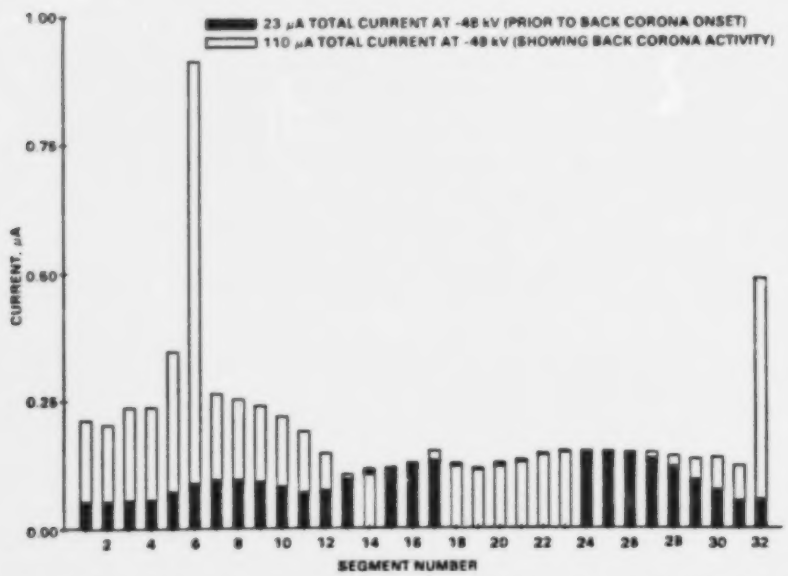

Fig. 12. Current distributions on the ash-covered plate for the ballasted wire electrode at 150°C.

In an effort to determine the conditions that initiate and sustain back-corona, a 1.6 cm diameter smooth, polished rod was overlayed with removable barbs. This electrode configuration was placed over the ash-covered collector plate, and the entire setup was heated to 100°C where ash resistivity was sufficiently high (mid 10^{11} ohm-cm) for back corona to occur. The barbs served as intense corona emission sources at applied voltages of −26 and −40 kV. Vigorous back-corona activity was induced on the ash layer opposite these corona sources. The barbs were lifted off the corona assembly while maintaining the same applied potential on the 1.6 cm rod. Immediately upon cessation of the primary corona from the barbs the back-corona activity extinguished. This experiment indicates that electric field strengths such as are found in ESP's are not sufficient by themselves to generate or even sustain back-corona activity. Primary current must be applied above a critical onset value for back-corona to occur.

Experiments were conducted to determine if the critical current density for back-corona onset could be quantified. The synergic relations between corona emission and back-corona discharges indicate that the local current densities must be well-known in order to make this determination. For this reason, pulsed energization and ballasted electrodes were used in these experiments. Each technique produced a uniform current distribution [8].

The importance of current uniformity was emphasized by comparing the value of total current required to initiate back-corona activity from a pulsed and a d.c. energized wire. The comparison was made with the same electrode arrangement, ash-layer thickness, and ash resistivity in both cases. The pulsed electrode, with a glow-discharge, achieved a total current greater than the electrode with d.c. energization, which had corona from discrete spots. The total current densities for the two corona systems were not indicative of the maximum local current densities at the ash layer. This observation has significant implications for the design of discharge electrodes in ESP's. The maximum useful current density will increase proportionately to the uniformity of the corona discharge. The statistical description of corona discharge uniformity in terms of the COV is inversely related to the limit of useful current density achievable in the presence of ash having a given resistivity. It is therefore a quantity which should be evaluated in the selection of corona electrodes, especially where high resistivity ash is to be collected.

The ash layer became rough with the continuing occurrence of back-corona. Ash was lifted physically from the surface of the layer in the regions of back-corona activity. The rough areas of the layer served as stationary locations for back-corona, as did other surface defects in the ash, such as craters formed by arcs. These stable sites sometimes became very intense, extinguishing nearby activity. Often these intense spots of back-corona did not produce radial streamers, but had plate-to-wire streamer propagation typical of positive corona. Several of these stable back-corona sites can be seen in the photograph presented in Fig. 7. The ash layer was also dis-

coloured by back-corona activity. In an effort to determine if any chemical or physical changes had occurred in the ash subjected to back-corona, scanning electron microscopy and elemental analyses were performed. Results of these analyses on samples exposed to various test conditions revealed no definite physical or chemical changes in the ash.

Observations were made of a section of collector plate removed from an ESP with its electrostatically deposited ash layer intact. The appearance and behaviour of the back-corona observed on this ash layer was essentially the same as that observed on the hand-smoothed ash layer. The surface of the electrostatically deposited ash layer, however, remained unaltered by continuous back-corona activity.

Hand-deposited ash layers of 0.32, 0.64, and 0.96 cm thicknesses were studied. The distribution and appearance of the back-corona produced was independent of the thickness of the layers. The effect of ash layer thickness on the *V—I* characteristics for the 0.32 cm wire is shown in Fig. 13. The increased resistance resulting from thicker ash layers affected the conditions for back-corona onset due to the different voltage drop across the layer. Once back-corona was initiated, the intensity of the discharge showed no dependence on ash-layer thickness.

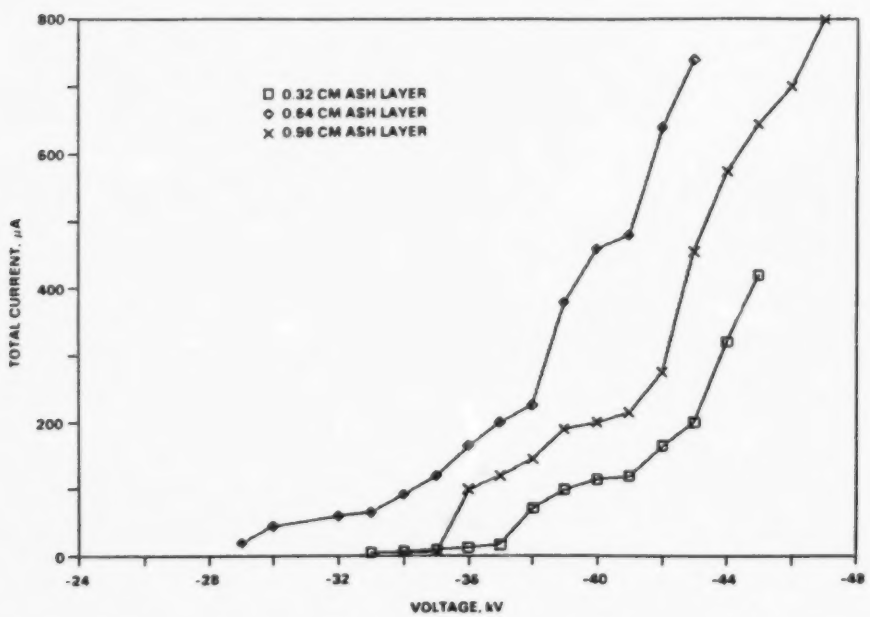

Fig. 13. The effect of ash layer depth on voltage-current characteristics of a 0.32 cm diameter wire at 150°C.

The effect of the back-corona in altering V—I curves and degrading particle charging is well known. Measurements of the effects of back-corona on the magnitude and distribution of current supplemented by visual observations of the character and behaviour of back-corona emissions have yielded information fundamental to the selection of discharge electrodes and operating voltage and current levels in ESP's collecting high resistivity ash.

Acknowledgements

This work was sponsored by the Industrial Environmental Research Laboratory of EPA under the direct guidance of Dr. Leslie E. Sparks (Co-operative Agreement No. CR-808973-01).

References

1 H.J. White, Industrial Electrostatic Precipitation, Addison-Wesley, Reading, MA, 1963, pp. 294 ff.
2 S. Masuda, A. Mizuno and K. Akutsu, Initiation condition and mode of back discharge for extremely high resistivity powders, IEEE 1977 IAS Conf., Printcraft, Inc., Conneaut, OH.
3 H.J. White, Industrial Electrostatic Precipitation, Addison-Wesley, Reading, MA, 1963, pp. 294 ff.
4 H.W. Spencer, III, Electrostatic Precipitators: Relationship Between Resistivity, Particle Size, and Sparkover. EPA-600/2-76-144 (NTIS PB257130), U.S. EPA, Research Triangle Park, NC, 1976.
5 S. Masuda and A. Mizuno, Initiation condition and mode of back discharge. J. Electrostat., 4 (1977/1978) 35—52.
6 J.R. McDonald, R.B. Mosley, and L.E. Sparks, An approach for describing electrical characteristics of precipitated dust layers. APCA J., 30 (4) 1980 372—376.
7 L.C. Thanh, Back-corona, Part I: its formation. J. Electrostat., 4 (1979) 139—160.
8 P.V. Bush and T.R. Snyder, Laboratory analyses of corona electrodes. J. Electrostat., 19 (1987) 83—99.
9 IEEE Standard Number 548-1981.
10 A.S.C. Ehrenberg, Data Reduction — Analysing and Interpreting Statistical Data. John Wiley and Sons, Chichester, England, 1975, pp. 176 ff.
11 L.B. Loeb, Electrical Coronas: Their Basic Physical Mechanisms. Univ. of Calif. Press, Berkeley, CA, 1965.
12 P. Lausen, H.H. Petersen, and H.J. Joergensen, Theory and application of pulse energization, Proc. International Conf. on Electrostatic Precipitation, EPRI/IGCI/APCA, 1981, pp. 531—555.

This document has been reviewed in accordance with U.S. Environmental Protection Agency policy and approved for publication. Mention of trade names or commercial products does not constitute endorsement or recommendation for use.

This article documents research that was conducted under the auspices of the U.S. Environmental Protection Agency (USEPA). As an arm of the government, the USEPA has a paid up, non-exclusive, irrevocable, worldwide license to reproduce, prepare derivative works, and distribute to the public all of the material contained herein, and to grant others acting on its behalf the right to do so. The USEPA grants to the National Technical Information Service, Department of Commerce, the right to act as its agent in the distribution of this material.